On the Structure and Bonding of First Row Transition Metal Ozone Carbonyl Hydrides

Gerhard A. Venter,† Helgard G. Raubenheimer, and Jan Dillen*

Department of Chemistry and Polymer Science, University of Stellenbosch, Private Bag X1, Matieland 7602, South Africa

Received: April 26, 2007; In Final Form: June 13, 2007

Model complexes of the general form $M(CO)_m(H)_n(O_3)$ ($m = 1-5$, $n = 0$ or 1) between ozone and the transition metals Ti to Cu were studied by density functional theory (DFT) calculations. The CDA charge decomposition method was used to analyze the interaction between the metal atom and the ozone ligand in terms of the traditional donation−back-donation mechanisms. Information about bond strengths was extracted from an analysis of the electron density in terms of the theory of atoms in molecules (AIM). The bonding in the ozone−metal complex was also studied within the NBO paradigm. Bond dissociation energies were calculated to be positive for all the complexes studied. Considering all the criteria employed in this study to analyze the interaction between the ozone and the transition metal, the Fe−complex is predicted to be the most stable, whereas the copper complex has the weakest metal−ozone interaction.

I. Introduction

Ozone is an unstable, blue, diamagnetic gas with a very characteristic metallic odor. In fact, the name ozone comes from the Greek word *ozein*, which means "to smell". The electronic structure of ozone has received a fair amount of attention in the computational chemistry literature, in particular referring to the performance of multireference methods. Various authors[1−11] have given good accounts of the electronic structure of ozone, not only in its open form (C_{2v}) but also in its cyclic form (D_{3h}). Popular methods have been many-body perturbation theory,[4] complete active space self-consistent field (CASSCF),[2,11] configuration interaction with singles and doubles (CISD),[6,8,10] more elaborate CI methods[5] coupled cluster theory with singles and doubles (CCSD)[4,6] and perturbation estimates of triples (CCSD(T)).[4,6,9] Density functional theory has also been applied to the problem.[7]

Aside from its fundamental importance in atmospheric chemistry, i.e., a strong absorbance in the dangerous ultraviolet region (λ_{max} 255.3 nm), it also exhibits a strongly oxidizing nature and associated tendency to transfer an oxygen atom with the production of dioxygen. Its acid reduction potential of 2.075 V is only exceeded by very potent oxidants such as fluorine, atomic oxygen and the OH radical, among others.[12] This destructive character of ozone is one of the reasons for the lack of stable structures of metal-containing compounds having ozone as a ligand. However, there do exist various examples of salts formed between anionic ozonide, O_3^-, and the group 1 alkali metals, e.g., LiO_3, KO_3, RbO_3, and CsO_3.[12]

This paper presents an investigation into the stability and bonding of selected first row transition metal series model complexes that contain ozone as ligand, in an attempt to predict the possibility and strength of such interactions in these still nonexisting compounds.

There have been very few previous reports on this specific problem. Flemming et al.[13] recently calculated the stabilization of O_3 in cyclic form by formation of a transition metal complex. Their calculations, using group 6 and 7 metals, were a continuation of earlier attempts by Sung and Hoffmann[14] on trioxygen (and thiozone) in various forms.

Our aim was to investigate whether complexes of this nature would have significant stability and, hence, in principle, could eventually be synthesized in the laboratory.

II. Computational Details

Density functional calculations (DFT) were carried out with Gaussian 98[15] and Gaussian 03[16] using the B3LYP hybrid density functional.[17] The 6-31G(d) basis set was used to describe the lighter atoms. For the metals, pseudopotentials were applied in the form of the Los Alamos effective core potentials with a double-ζ basis set for the valence shell electrons (LANL2DZ).[18] Complexes were optimized on a symmetry-unconstrained energy surface and the resulting stationary points characterized by analysis of the vibrational frequencies.

Closed shell species, such as O_3 in this case, are normally calculated by means of spin restricted theory. However, allowing the spin restricted determinant to become unrestricted can, at least in principle, lead to a lower energy solution. A solution to the SCF procedure is externally unstable if the energy can be lowered by relaxing some of the initial constraints, such as spin (i.e., restricted or unrestricted) or spatial/orbital symmetry. Bauernschmitt and Ahlrichs[19] have extended the initial work of Seeger and Pople[20] and define methods for testing solutions to DFT problems for such instabilities. Ozone is a typical candidate for the employment of multireference methods, and including d-metals in the calculations increases the need for a capable description of nondynamic correlation to minimize the possibility of spin contamination. Wave functions of complexes with incomplete d-electron valence shells were thus always tested for instabilities, and if this turned out to be the case, the wave functions were reoptimized, allowing for a lower energy

* To whom correspondence should be addressed. E-mail: jlmd@sun.ac.za.
† Current address: Department of Chemistry, University of Cape Town, Private Bag X3, Rondebosch 7701, South Africa.

10.1021/jp0732256 CCC: $37.00
Published on Web 07/28/2007

SCHEME 1: Selected Occupied (7−12) and Virtual (13) Molecular Orbitals of C_{2v} Ozone[a]

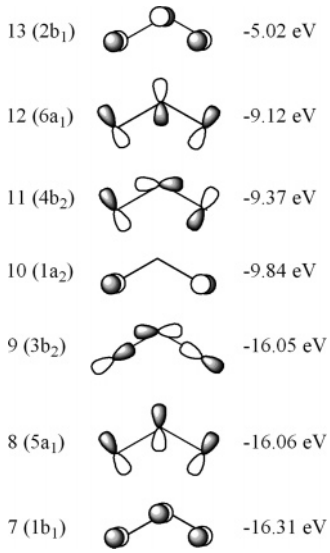

[a] The assigned symmetry is relative to the *z*-axis lying in the molecular plane, with the C_2-axis. Orbitals 10 (HOMO-2) to 12 (HOMO) have energies similar to the accepting orbitals on the metal. Orbital 13 is the LUMO.

SCF solution. Only complexes with the lowest possible spin multiplicity were considered in this study.

Atomic partial charges were calculated using the NBO 3.1 program package,[21,22] included with the Gaussian 98 code, and this program was also used to carry out the NBO analysis.

The electron density topology of the complexes was investigated within the paradigm of atoms in molecules (AIM).[23] The AIMPAC suite of programs was used in this regard.[24]

Bonding in transition metal complexes is often described in terms of σ-donation and π-back-donation, based on the Dewar−Chatt−Duncanson model.[25,26] According to this theory the ligand donates electron density into the valence orbitals of the metal, which responds by releasing some of its negative charge through donation into, for example, the unoccupied π^* orbital of the ligand using filled d-orbitals of correct symmetry. The ability of ozone to live up to this mechanism has, to our knowledge, not been investigated.

Donation and back-donation in the complexes were explored by using the charge-decomposition analysis (CDA) of Dapprich and Frenking.[27,28] In this method the complex orbitals are described by a linear combination of properly chosen fragment orbitals in the geometry of the complex, resulting in a quantitative expression for the donation, d_i, and back-donation, b_i involving the *i*th molecular orbital. Contributions by occupied/occupied and unoccupied/unoccupied combinations are given by repulsive polarization and rest terms, respectively.

III. Results and Discussion

Structure of $M(CO)_m(H)_n(O_3)$. Scheme 1 presents the molecular orbitals of ozone, calculated at B3LYP/6-31G(d), with the corresponding energy levels. Ozone has the ability to coordinate as a π-electron donor with metal orbitals, utilizing four electrons. It only has two (partially) occupied π-orbitals in the valence region, $2b_1$ and $1a_2$. It could also bind as a bidentate σ-donor. In this case coordination would occur by means of the two terminal oxygens and again four electrons are involved, $6a_1$ and $4b_2$. Of course, the ozone ligand can also bind by coordination of only one terminal oxygen atom. Possible coordination geometries were explored by optimizing four

SCHEME 2: Four Possible Coordination Geometries for the Metal−Ozone Complexes

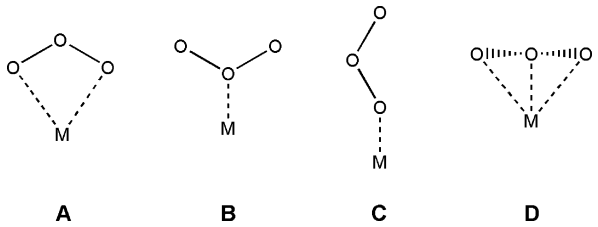

different starting geometries of one ozone ligand relative to an otherwise bare metal ion (Scheme 2), the whole "complex" having an overall charge of +2. First, the ozone ligand was placed in the most likely orientation for η^2-coordination (type **A**), with the two terminal oxygen atoms at equal distances to the metal, and all four atoms in a plane. Second and third, the central (type **B**) or terminal oxygen (type **C**) was placed closest to the metal to respectively allow for η^1-coordination. Finally, the ozone ligand was arranged to approach the metal with three equidistant oxygens (η^3-coordination), type **D**. As can be expected, more than one of the different starting geometries converged to the same final structure. In some instances, converged structures had negative frequencies which, upon following the corresponding eigenvector, led to other geometries (i.e., coordination numbers) being a minimum on their respective potential energy surfaces. The lack of an appropriate ligand field leads to significant degeneracy among the d-orbitals in these complexes. This introduces the possibility of high degrees of spin contamination in restricted wave functions resulting in RHF/UHF instabilities. These were treated as mentioned earlier.

Inspecting the molecular orbitals of ozone given in Scheme 1, one might have expected planar bidentate coordination to be most common, as the HOMO to HOMO−2 orbitals with energies similar to those expected of the accepting metallic orbitals[13] are orientated in such a way as to maximize orbital overlap. This expectation is indeed confirmed by the calculations, according to which Ti^{2+} and Co^{2+} afford type **D** geometries, V^{2+}, Cr^{2+}, Mn^{2+}, and Fe^{2+} type **A** geometries, and Ni^{2+} and Cu^{2+} type **C**. Type **B** geometry is not observed. A simple explanation for this could be repulsion between the positive charge on the metal and that of the central oxygen of ozone. These results suggested that an **A**-type coordination could be used as the starting geometry for further calculations.

Subsequent calculations were carried out on larger complexes of the general composition $M(CO)_m(H)_n(O_3)$, with M = Ti, V, Cr, Mn, Fe, Co, Ni, and Cu. The values of *m* and *n* were determined by invoking the 18-electron rule and classifying O_3 as a four-electron donor, CO as a two-electron donor and H as a one-electron donor. The metal atoms were considered to be electrically neutral. Because both the ozone and carbonyl ligands donate an even number of electrons, the hydrogens are used to compensate for metals with an uneven number of valence electrons. Selected structural parameters of the optimized geometries are given in Table 1. Figure 1 shows the final calculated structures. All the complexes can be described as having type **A** ozone coordination.

Two different metal−carbonyl bond distances are found for the $Ti(CO)_5(O_3)$ (**1**) complex. Two cis-oriented carbonyls have Ti−CO bonds of 2.124 Å, whereas the other two are longer (2.156 Å). An interesting feature is the distortion of the carbonyl occurring trans to the ozone ligand. It forms an angle of 163° with the metal and central oxygen of the ozone and has a much larger Ti−C bond length of 2.252 Å. The ozone ligand is staggered with respect to the four carbonyls cis thereto. In the

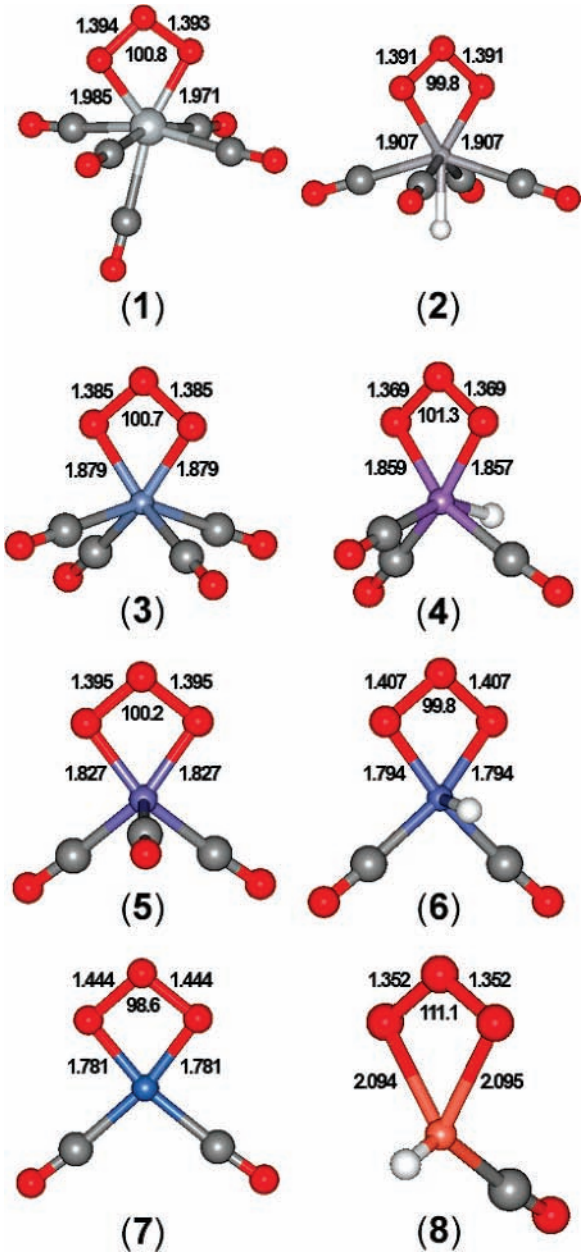

Figure 1. Optimized structures of $M(CO)_m(H)_n(O_3)$ complexes. M = Ti (**1**), V (**2**), Cr (**3**), Mn (**4**), Fe (**5**), Co (**6**), Ni (**7**), Cu (**8**). Also shown are the O−O and M−O bond lengths (Å) and the O−O−O angle (deg).

vanadium complex, $V(CO)_4H(O_3)$ (**2**), the structure with the hydrogen trans to the ozone ligand is the most stable. The V−CO bond distances are all equal (2.010 Å). The $Cr(CO)_4(O_3)$ (**3**) complex features two slightly different Cr−CO bond lengths of 1.939 Å and 1.923 Å for each of the two CO ligands trans to each other in a square pyramidal arrangement. The $Mn(CO)_3(H)(O_3)$ complex (**4**) was built with the hydrogen trans to the ozone ligand but rotated in the optimization into a cis configuration. Two of the Mn−CO bonds are nearly similar (1.856 Å), and the third, approximately trans to the hydrogen atom, is 1.848 Å. The Fe−CO separation in $Fe(CO)_3(O_3)$ (**5**) is 1.780 Å for the carbonyl perpendicular to the plane of the ozone ligand and 1.846 Å for the remaining two. These two ligands are both 12° out of the plane that contains the ozone oxygen atoms. Two stationary points were found for the $Co(CO)_2(H)(O_3)$ complex (**6**). One structure (shown in Figure 1) has the ozone ligand in-plane with the carbonyls, in the other the ligand is slightly perturbed out of the plane. Interestingly though, the in-plane geometry is 3.5 kcal/mol more stable and for this structure the Co−CO bonds are 1.854 Å. The hydrogen lies 10° from the normal to the ozone−carbonyl plane. The $Ni(CO)_2(O_3)$ complex (**7**) optimized to a planar structure with Ni−CO bond lengths of 1.881 Å. In the $Cu(CO)(H)(O_3)$ complex (**8**) the Cu−CO bond distance is 1.949 Å with the hydrogen and carbonyl lying perpendicular to the ozone plane.

Our analysis of the interaction starts with comparison of the average of the two shortest M−O distances in each complex. Taking into account the different metal radii, one can interpret this distance as a guide to the relative bond strength. With the exception of Ti and V, which has metal radii of 1.47 and 1.34 Å, respectively, the first row metals all have radii between 1.26 and 1.28 Å. On this basis these distances should provide a reasonable guide of bond strength, possibly with the exception of Ti and V. With the bond length inversely proportional to the strength of the interaction, the trend in the latter is

Cu (**8**) < Ti (**1**) < V (**2**) < Cr (**3**) < Mn (**4**) < Fe (**5**) < Co (**6**) < Ni (**7**)

Except for complex **8**, this trend follows the row order exactly, including Ti and V. Owing to the design considerations of our hypothetical complexes, the number of carbonyl ligands decreases in response to the increase in metallic d-orbital occupation, as one moves along the row order. This introduces less sterical hindrance, as is also evident by the carbonyl to metal separation distances, which decrease along the row order. Compare in this regard also the structures given in Figure 1: one clearly notices the angle between the terminally bonded oxygen and a particular carbonyl ligand increasing as the total number of ligands decreases, further decreasing electron pair repulsion. Although important, bonding in complexes is not exclusively determined by radially dependent contributions (i.e.,

TABLE 1: Selected Structural Parameters of Optimized $M(CO)_m(H)_n(O_3)$ Complexes[a]

	1, $Ti(CO)_5(O_3)$	**2**, $V(CO)_4(H)(O_3)$	**3**, $Cr(CO)_4(O_3)$	**4**, $Mn(CO)_3(H)(O_3)$
M−O(1)	1.985	1.907	1.879	1.859
M−O(3)	1.971	1.907	1.879	1.857
O(1)−O(2)	1.394	1.391	1.385	1.369
O(1)−O(3)	1.393	1.391	1.385	1.369
O(1)−O(2)−O(3)	100.8	99.8	100.7	101.3
	5, $Fe(CO)_3(O_3)$	**6**, $Co(CO)_2(H)(O_3)$	**7**, $Ni(CO)_2(O_3)$	**8**, $Cu(CO)(H)(O_3)$
M−O(1)	1.827	1.794	1.781	2.095
M−O(3)	1.827	1.794	1.781	2.094
O(1)−O(2)	1.395	1.407	1.444	1.352
O(1)−O(3)	1.395	1.407	1.444	1.352
O(1)−O(2)−O(3)	100.2	99.8	98.6	111.1

[a] Distances in Ångstrom, angles in degrees.

TABLE 2: Natural Atomic Partial Charges of $M(CO)_m(H)_n(O_3)$[a]

	1, $Ti(CO)_5(O_3)$	**2**, $V(CO)_4(H)(O_3)$	**3**, $Cr(CO)_4(O_3)$	**4**, $Mn(CO)_3(H)(O_3)$
$q(O_1)$	−0.314	−0.267	−0.253	−0.241
$q(O_3)$	−0.334	−0.267	−0.253	−0.239
$q(O_2)$	0.055	0.054	0.066	0.104
$q(\Sigma O_n)$	−0.593	−0.479	−0.440	−0.375
M	−0.317	−0.608	−0.464	−0.312
	5, $Fe(CO)_3(O_3)$	**6**, $Co(CO)_2(H)(O_3)$	**7**, $Ni(CO)_2(O_3)$	**8**, $Cu(CO)(H)(O_3)$
$q(O_1)$	−0.325	−0.345	−0.426	−0.336
$q(O_3)$	−0.325	−0.345	−0.426	−0.336
$q(O_2)$	0.061	0.054	0.001	0.217
$q(\Sigma O_n)$	−0.589	−0.724	−0.852	−0.456
M	0.086	0.396	0.705	0.799

[a] Charges in e.

distances). Therefore, care should be taken to conclude that this trend does provide a reliable measure of interaction strength.

Structures with identical or near-identical (in the case of **1**) ozone O−O bond lengths and M−O ligand bond distances were obtained for all complexes. It has to be kept in mind that because the complexes have been optimized without enforcing symmetry constraints, an exactly symmetrical final structure is unlikely, and therefore some allowance needs to be made regarding a structure as symmetric. The O−O bond length remains in the region of 1.37−1.40 Å in **1** to **6**. The bond becomes considerable longer in complex **7**, a likely consequence of increased electron pair repulsion present due to planarity. The O−O−O angle also remains around 100.2 ± 1.6° for all compounds but the highly unsymmetrical **8**. Overall though, complexation of the ozone to the metal atom results in a ±0.1 Å lengthening of the O−O bonds and a significant reduction of the O−O−O angle by ±18°. The change in O−O−O angle is easily rationalized in terms of the bidentate coordination, which forces the donor atoms together; that the 0.1 Å change in O−O bond lengths is solely due to coordination warrants further investigation.

An explanation for this might be found by investigating the back-donation by the filled metal orbitals into the antibonding π^* orbital of ozone. It has already been shown that the lengthening of the AB multiple bond in the transition metal complexes L_nM-AB can be attributed to electron back-donation from the metal to the π^* orbital of AB.[29] That will be discussed together with the charge decomposition analysis in a later section.

However, the changes mentioned might also be an indication of a change in the electronic structure of ozone. Reduction of the ozone to ozonide appears to be a reasonable explanation, surely more so if only regarded on an experimental level due to its high reduction potential. Of course, reduction of ozone is possible to either O_3^- or O_3^{2-}. The experimental O−O bond distance in radical O_3^- is 1.34 ± 0.03 Å and the O−O−O angle is 112.6 ± 2°.[30a] Similar data for the O_3^{2-} anion are unavailable. For the free ozone molecule, the corresponding values are approximately 1.272 Å for the distance and 116.7−117.8° for the angle.[30b−d] In the absence of experimental O_3^{2-} data, it is worthwhile to compare the bond distances with the dioxygen series: 1.12, 1.21, 1.28, and 1.49 Å going from O_2^+ to O_2, O_2^-, and O_2^{2-}.[31] It is thus clear that reduction (placing electrons in antibonding orbitals) lengthens the O−O bond length, which in ozone will then lead to an increase in the bond angle.

The above, somewhat superficial, observations indicate that metal oxidation and concurrent ozone reduction should also be considered an outcome of the interaction. Analysis of the bonding, specifically with regard to donation and back-donation, needs an accurate estimation of the electron count on both the ligand and metal center. The importance of this will become clear in the next section, and our attention now shifts to this problem.

Electron Count on M and O_3. The formal charges considered for the compounds in this study are ideally a neutral ligand and neutral metal, or a charge of −2 for the ligand and +2 for the metal, without taking the hydrides into account. A good and straightforward guideline for such assignment is examining the atomic partial charges on the O_3 ligand. Charges calculated from the natural population analysis (NPA) are shown in Table 2. For the free ozone molecule, B3LYP/6-31G(d) values of −0.116 e on the terminal oxygens and 0.231 e on the central oxygen are found. For the free ozonide ion, the corresponding values are calculated to be −0.833 e and −0.330 e, respectively. As can be seen from Table 2, the sum of charges on the ozone molecule in its complexed form varies between −0.375 e and −0.852 e, depending on the specific complex. The central oxygen has a relatively low partial positive charge with the terminal oxygen atoms carrying a large partial negative charge, just as is the case in free ozone. Hence, it is clear that despite the assumed dative coordination, the ozone ligand still carries a net negative charge in each of the complexes. In the only comparable previous computational study on complexes of this kind, Flemming et al. calculated Mulliken charges on the O_3 ligand to be around −0.7 e, in accordance with our results, and reasoned that this indicates some ozonide character in the ligand.[13]

Shifting our attention to the metallic centers, a periodic trend is once again noted—negative partial charges are found on the Ti, V, Cr, and Mn atoms. The charge on the Fe atom is close to zero, whereas the charges on the remaining Co, Ni, and Cu atoms are positive (see Table 2). These charges represent the interplay between donation by all the ligands, which *increases* the metal electron charge, and back-donation from the filled metal d-orbitals which *decreases* the electron population. Little information can thus be gathered with respect to the ozone coordination specifically. However, this subject will be discussed in the next section and for the moment we concentrate on assignment of formal oxidation states. A breakdown of the metal population in terms of 3d and 4s (natural) orbitals is given in Table 3. For comparison, similar data were also calculated for the carbonyl complexes $Cr(CO)_6$ (**3b**), $Fe(CO)_5$ (**5b**), and $Ni(CO)_4$ (**7b**). In these complexes the NPA charges on the metals are −1.487 e for $3d^{6.98}4s^{0.49}$ in **3b**, −0.561 e for $3d^{8.09}4s^{0.47}$ in **5b**, and 0.285 e with a $3d^{9.23}4s^{0.47}$ configuration in **7b**. In all these complexes the metal has an oxidation state of zero. Complexes **3**, **5**, and **7** all have significantly less d-orbital occupation and more positive metal partial charges, from which we conclude that even more negative charge is transferred to

TABLE 3: Metal Atomic Orbital Populations of $M(CO)_m(H)_n(O_3)$

	1, $Ti(CO)_5(O_3)$	**2**, $V(CO)_4(H)(O_3)$	**3**, $Cr(CO)_4(O_3)$	**4**, $Mn(CO)_3(H)(O_3)$
Σ(3d)	3.86	5.20	6.04	6.87
4s	0.41	0.39	0.40	0.42
	5, $Fe(CO)_3(O_3)$	**6**, $Co(CO)_2(H)(O_3)$	**7**, $Ni(CO)_2(O_3)$	**8**, $Cu(CO)(H)(O_3)$
Σ(3d)	7.48	8.12	8.80	9.67
4s	0.42	0.45	0.43	0.48

TABLE 4: Results of the Charge-Decomposition Analysis between Neutral O_3 and $M(CO)_mH_n$ in Terms of Donation, d, Back-Donation, b, Repulsive Polarization, r, and the Rest Term, Δ

	1, $Ti(CO)_5(O_3)$	**2**, $V(CO)_4(H)(O_3)$	**3**, $Cr(CO)_4(O_3)$	**4**, $Mn(CO)_3(H)(O_3)$
d	0.462	0.477	0.440	0.237
b	0.188	0.192	0.147	−0.012
r	−0.395	−0.421	−0.328	−0.113
Δ	0.021	0.014	0.077	0.230
	5, $Fe(CO)_3(O_3)$	**6**, $Co(CO)_2(H)(O_3)$	**7**, $Ni(CO)_2(O_3)$	**8**, $Cu(CO)(H)(O_3)$
d	0.494	0.305	0.331	0.353
b	0.159	−0.012	−0.020	0.107
r	−0.353	−0.065	−0.042	−0.157
Δ	0.034	0.204	0.173	0.005

TABLE 5: Results of the Charge-Decomposition Analysis between O_3^{2-} and $[M(CO)_mH_n]^{2+}$ in Terms of Donation, d, Back-donation, b, Repulsive Polarization, r, and the Rest Term, Δ

	1, $Ti(CO)_5(O_3)$	**2**, $V(CO)_4(H)(O_3)$	**3**, $Cr(CO)_4(O_3)$	**4**, $Mn(CO)_3(H)(O_3)$
d	0.750	0.809	0.796	0.738
b	−0.007	−0.035	−0.014	−0.007
r	−0.408	−0.461	−0.394	−0.332
Δ	−0.059	−0.051	−0.052	−0.056
	5, $Fe(CO)_3(O_3)$	**6**, $Co(CO)_2(H)(O_3)$	**7**, $Ni(CO)_2(O_3)$	**8**, $Cu(CO)(H)(O_3)$
d	0.759	0.789	0.765	0.477
b	−0.022	−0.002	0.001	0.001
r	−0.352	−0.305	−0.284	−0.110
Δ	−0.051	−0.051	−0.042	−0.060

ozone than to the CO ligands above, thus speaking for, at least partially, metal oxidation and ozone reduction toward ozonide.

As a side note, for all complexes, except **1**, the best representation of a Lewis structure ("best" in terms of the NBO formalism) calculated by the NBO program corresponds to a noncovalent, ion pair adduct $M(CO)_mH_n^{\delta+}\cdots O_3^{\delta-}$. In other words, formal natural bond orbitals are not calculated between the metal−carbonyl fragment and the ozone. More on this result will be discussed in a later section.

Donation and Back-Donation in $M(CO)_m(H)_n(O_3)$. Before the computational results are presented, we first consider from a qualitative molecular orbital viewpoint whether the electronic structure of ozone allows a donation/back-donation bonding mechanism. The LUMO of O_3 is a π-orbital and could, at least in principle, facilitate π-acidity (cf. Scheme 1). The LUMO of O_3^{2-}, however, consists of out-of-phase contributions from the in-plane p-orbital lying along the O−O bond axis of the terminal oxygens and the perpendicular, but also in-plane, p-orbital of the central oxygen. This would only allow σ-overlap with the d-orbitals of the metal fragment and (π-) back-donation is impossible.

The bonding in the various compounds was investigated within the framework of the Dewar−Chatt−Duncanson (DCD) model[25,26] by means of charge-decomposition analysis (CDA) of Dapprich and Frenking.[28] The analysis was first done with O_3 and $M(CO)_mH_n$ as the two fragments, and then also with O_3^{2-} and $M(CO)_mH_n^{2+}$. Results are shown in Table 4 and Table 5, respectively. The rest term, Δ, represents overlap between empty orbitals on the metal fragment and empty orbitals on the ligand. Relaxation due to such overlapping is meaningless, and it has been found a good indicator for classifying the complex as a donor−acceptor complex or not.[32] If the term differs greatly from zero, this is an indication that the two fragments specified as input are not closed-shell, but rather two open-shell fragments interacting to form a covalent bond. As seen from Table 4, complexes **1**, **2**, **3**, **5**, and **8** all have rest terms close to zero. However, **4**, **6**, and **7** have significantly large rest terms accompanied by large unphysical negative values of back-donation, *b* (in fact, this is further indication of regular donation, not back-donation, as was intended through the fragment specification). On the other hand, it is seen from Table 5 that if the O_3 ligand is considered as an ozonide (O_3^{2-}), all complexes have rest terms close to zero. In the latter case, no back-donation occurs, as is expected from the qualitative inspection of the molecular orbitals mentioned earlier.

For a few more detailed observations, we first concentrate on the ozone complexes summarized in Table 4. The complexes with rest terms near zero and hence for which the DCD framework holds, all have donation and back-donation values of similar magnitude (between 0.440 and 0.494), except for the Cu complex, **8**. This complex has already been identified to contain anomalous bonding on the basis of its unsymmetrical structure. Whereas the average $M-O_3$ bond length decreases along the series Ti to Ni, the values of the donation or back-donation show no such correlation. The ozone in complex $Fe(CO)_3(O_3)$, **5**, appears to be the best acceptor whereas the highest amount of back-donation occurs in the vanadium complex $V(CO)_4H(O_3)$, **2**. For those complexes where the rest term is close to zero and a donation/back-donation description holds,

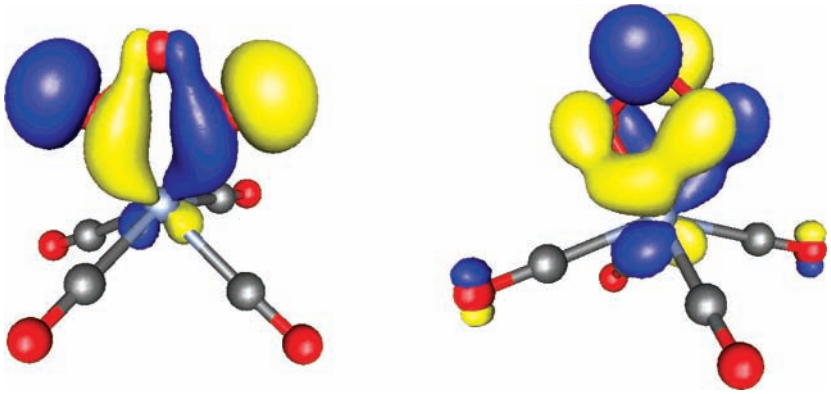

Figure 2. Molecular orbitals 43 (left) and 46 (right) of $Cr(CO)_4(O_3)$ contributing most to the total donation term, according to charge decomposition analysis.

repulsive polarization is large and negative, indicating a removal of electron density from the occupied/occupied orbitals of the fragments.

In Table 5 complex **8** again shows different donation and back-donation values compared to the others. In this description, $V(CO)_4H$ is the best acceptor (albeit only marginally over Cr and Co). Because, as mentioned earlier, back-donation is of no importance here, it might be surprising that a relationship between the relative amount of donation and M−O bond lengths does not exist. In a previous CDA study undertaken among others by the originators of the CDA method,[29] the authors have considered complexes of similar structures to those we have studied, e.g., $M(CO)_5L$ and $M(CO)_3L$. Their conclusion is that the amount of charge donation and back-donation between the metal and the chosen ligand should not be used as a measure of the bond strength, especially if the complexes compared are not similar in structure.

No apparent reason exists to expect a fundamentally different bonding mechanism in **4**, **6**, and **7** (especially given the periodic trends seen in bond lengths for instance); hence, overall, the breakdown of the CDA analysis also points to a description in which the ozone is, at least partially, reduced upon complexation.

Of course, the other ligands, which have been chosen for reasons of the computational benefit to lift the degeneracy of the d-orbitals and to ease calculation convergence, also affect the electron rearrangement in the complexes to a considerable extent. The effect of the CO and H ligands is best illustrated by the NPA charges (Table 2). The first four complexes carry four or more CO and H ligands in addition to the common ozone ligand, and all have negative atomic partial charges on the metal atom, indicating that donation by the ligands exceeds back-donation by the metal. The ozone ligand still carries a considerable negative charge and the positive charge required to uphold a total neutral charge on the complex is carried on the ligands, not the metal atom itself. This is a sound measure that donation exceeds acceptance by the non-ozone ligands.

Contributions to bonding by individual orbitals can also be investigated in the CDA breakup. Analysis of all the complexes reveals that σ-bonding can be described according to a general trend in all examples; that is, donation is dominated by two orbitals, having similar composition in all complexes. As representative of the bonding in these complexes, the molecular orbitals of $Cr(CO)_4(O_3)$ are considered. The two MOs participating largely in the donation terms are MOs 43 and 46, shown in Figure 2. Comparing these with the molecular orbitals of free ozone, it is clear that they result from overlap of the $4b_2$ and $2b_1$ ozone MOs and d-orbitals of the metal center. The $4b_2$ MO is the out-of-phase lone pairs on the terminal oxygens, directed toward the metal center. The $2b_1$ MO is higher in energy and is the one that becomes occupied upon reduction of O_3, consisting of the in-phase lone pairs on the terminal oxygens and lying perpendicular to the ozone molecular plane. This analysis confirms the four-electron bonding of the O_3 moiety and also shows the involvement of a reduced form. It is also interesting to note that Flemming et al. reported an energy mismatch between the donor orbitals of O_3 (*too low* in energy) and the acceptor orbitals of their chosen metallic fragment, $W(CO)_3$.[13] Therefore, they replaced the CO ligands with isoelectronic NO^+ ligands. In our case, the higher energy $2b_1$ MO of ozone becomes available for coordination overlap, effectively through reduction of the moiety, which might also solve the problem of a mismatch intrinsically. In conclusion, and referring to ozonide ligands as in Table 5, the order of increasing L → M donation is

$$\text{Cu (}\mathbf{8}\text{)} < \text{Mn (}\mathbf{4}\text{)} < \text{Ti (}\mathbf{1}\text{)} < \text{Fe (}\mathbf{5}\text{)} < \text{Ni (}\mathbf{7}\text{)} < \text{Co (}\mathbf{6}\text{)} < \text{Cr (}\mathbf{3}\text{)} < \text{V (}\mathbf{2}\text{)}$$

Electron Density Analysis. In an attempt to further categorize the strength of interaction in the different complexes, an AIM analysis of the topology of the electron density at representative critical points was carried out. Owing to strictly adhering to the 18-electron rule, structural changes upon complexation should therefore be more important for the complexes with more ligands because of steric hindrance. Later we shall look at dissociation energies as a probe of stabilities; however, an intrinsic component of these values is structural deformation of the *whole system*, which becomes of increasing importance as the number of *total ligands* change. This problem can be overcome by using values that probe the instantaneous interaction, based on the electron density. Although CDA also analyzes instantaneous interactions, it is understandably influenced to a greater extent by additional ligands, because these also contribute significantly to the total donation and back-donation values.

Thus, calculation of the electron density at the bond critical points, $\rho_b(\mathbf{r})$, indicates that bonding of the ligand to the metal leads to a decrease of ρ_b(O−O) from 0.4532 e·bohr^{-3} in unbound ozone to between 0.3985 and 0.2876 e·bohr^{-3} in bound ozone. As a measure of the strength of the bonding interaction, the electron density values at the critical points of the M−O bond and the O−O interactions in the ligand, as well as the M−O−O−O ring critical point, can be used. Whereas an

TABLE 6: Electron Density Values at Important Critical Points of $M(CO)_mH_n(O_3)$[a,b]

	1, $Ti(CO)_5(O_3)$	**2**, $V(CO)_4(H)(O_3)$	**3**, $Cr(CO)_4(O_3)$	**4**, $Mn(CO)_3(H)(O_3)$
ρ_b(M−O)	0.0929/0.0953	0.1131	0.1197	0.1187/0.1194
ρ_b(O−O)	0.3271/0.3283	0.3300	0.3351	0.3497/0.3500
ρ_r(M−O−O−O−O)	0.0460	0.0515	0.0531	0.0544
	5, $Fe(CO)_3(O_3)$	**6**, $Co(CO)_2(H)(O_3)$	**7**, $Ni(CO)_2(O_3)$	**8**, $Cu(CO)(H)(O_3)$
ρ_b(M−O)	0.1286/0.1287	0.1361/0.1360	0.1389	0.0611/0.0610
ρ_b(O−O)	0.3267/0.3271	0.3169/0.3168	0.2876/0.2877	0.3985/0.3986
ρ_r(M−O−O−O−O)	0.0544	0.0554	0.0535	0.0359

[a] Values in e·bohr^{-3}. [b] In cases where the bond is unsymmetrical, values for both the bonds are given.

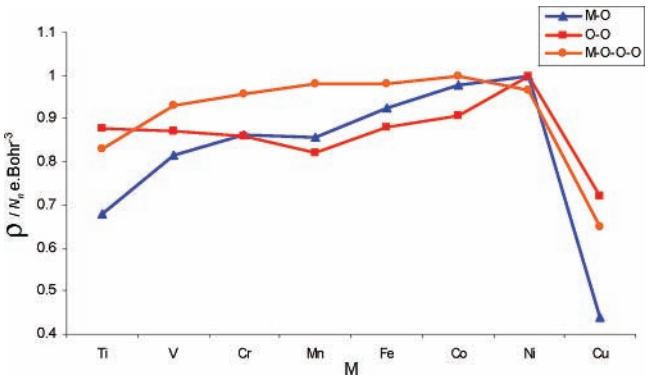

Figure 3. Electron density values at the M−O bond critical point, the inverse of the electron density at the O−O bond critical point and the M−O−O−O ring critical points of $M(CO)_m(H)_n(O_3)$c compounds; all values have been normalized between 0 and 1.

increase in ρ_b(M−O) signifies a stronger bond between the metal and O_3, a decrease in ρ_b(O−O) indicates the same. Table 6 contains the results, and a graphical trend is given in Figure 3. The respective trends, all signifying increasing interaction strength between the metal and O_3 are

ρ_b(M−O): Cu (**8**) < Ti (**1**) < V (**2**) < Mn (**4**) < Cr (**3**) < Fe (**5**) < Co (**6**) < Ni (**7**)

ρ_b(O−O): Cu (**8**) > Mn (**4**) > Cr (**3**) > V (**2**) > Ti (**1**) > Fe (**5**) > Co (**6**) > Ni (**7**)

ρ_r(M−O−O−O): Cu (**8**) < Ti (**1**) < V (**2**) < Cr (**3**) < Ni (**7**) < Mn (**4**) = Fe (**5**) < Co (**6**)

The electron density at the ring critical point, ρ_r(M−O−O−O), gives a slightly different picture. Here, Ni (**7**), which has the strongest interaction according to the other two indicators, moves down in the order. Mn (**4**), which lies low in the former trends, moves up considerably. Interpreting the three trends in general, the conclusion is that the strongest interaction occurs in Fe (**5**), Co (**6**), and Ni (**7**). These complexes also have the shortest M−O bonds.

The nature of the interaction also follows from AIM analysis. For this, the values of the energy density (H_b) at the M−O bond critical points were compared. It has been shown that a negative value of the total energy density, given as the sum of the kinetic and potential energy densities, indicates covalent or shared interaction, whereas positive values are indicative of an ionic or closed-shell interaction.[33] Complex **8** has a positive value of H_b (0.0089 hartree·bohr^{-1}), indicating a high degree of noncovalent interaction. This reaffirms its different bonding nature, as elucidated by all the previous measures of bond strength showing that it has a much weaker metal−ozone bond than the other complexes. Complexes **5**−**7** have similar negative values (−0.0439, −0.0479, and −0.0460 hartree·bohr^{-1}, respectively), as have **3** and **4** (−0.0323 and −0.0339 hartree·bohr^{-1}, respectively). Complex **2** has an energy density of less than half that of the highest value of the other complexes (−0.0188 hartree·bohr^{-1}). Complex **1** has a value close to zero (−0.0014 hartree·bohr^{-1}), indicating the considerably larger noncovalent character of this bond. A correlation can be drawn between the H_b values and the bond strengths as given by comparing ρ_b(M−O): more covalent character corresponds to a strengthening in the bond.

Natural Population Analysis. As mentioned earlier, the most probable structures (in terms of a Lewis interpretation) obtained by the NBO algorithm corresponds to an $M(CO)_mH_n^{\delta+}\cdots O_3^{\delta-}$ representation between closed-shell fragments. However, if needed, a specific Lewis structure can be assigned by hand,[21,22] at the cost of lower occupation of localized orbitals. It can be argued that assigning bond orbitals between the O_3 ligand and metal center could force some "artificial covalency" on the description, but given the findings in the previous section we believe this to be an acceptable side effect. Of course, bond orbtials are indeed calculated between the carbonyl ligands and the metal centers, this being the archetypal donor−acceptor interaction. We illustrate initial but representative results by considering $V(CO)_4H(O_3)$ as an example. Specifying the Lewis structure to ensure that M−O bond orbitals are calculated leads to a 0.4% increase in non-Lewis occupation, equal to just more than a full electron. Considering the $V(CO)_4H^{\delta+}\cdots O_3^{\delta-}$ partitioning identified as the most probable form if no explicit Lewis structure is specified, it consists of two units: an O_3 unit and a $V(CO)_4H$ unit. The O_3 unit is in fact a cyclic structure with single bonds between two pairs of oxygens with a common partner, O(1)−O(2) and O(1)−O(3). Two bond orbitals are found between O(2) and O(3), having very low occupancy (1.38 and 1.76 e), including two additional antibonding orbitals with very high (1.95 and 1.55 e) occupancy. This is a highly delocalized structure with little correspondence to isolated ozone, or with the structure expected from the bound state. Interaction between the O_3 unit and the $V(CO)_4H$ unit is seen in the second-order perturbation estimates of interaction between natural orbitals of the fragments. Of importance is the interaction between the oxygen atoms oriented closest to the metal fragment, O(2) and O(3), and the metal fragment. The second O(2)−O(3) bond orbital is found to interact with a lone pair orbital on the vanadium, as well as with low occupancy Rydberg orbitals of the vanadium and the carbonyl-carbon. Considerable delocalization into vanadium−carbon antibonding natural orbitals, as well as a large component into the vanadium−hydrogen antibonding NBO by both bonding and antibonding O(2)−O(3) NBOs are obvious. In addition, there are also some terms corresponding to interaction between all of the above-mentioned $V(CO)_4H$ bonding and antibonding orbitals and Rydberg NBOs on O(2) and O(3). Considerable delocalization thus occurs, both interfragmentally in the O_3 unit and intrafragmentally between the O_3 and $V(CO)_4H$ units. Delocalization between the O_3 unit

TABLE 7: NBO-Hybridization Information for the M−O Bond of $M(CO)_mH_n(O_3)$

	1, $Ti(CO)_5(O_3)$	**2**, $V(CO)_4(H)(O_3)$	**3**, $Cr(CO)_4(O_3)$	**4**, $Mn(CO)_3(H)(O_3)$
% M[a]	11.35	18.02	19.95	27.56
s/p/d[b]	11.62/7.87/80.51	20.90/0.19/78.91	14.11/0.85/85.03	16.7/0.05/83.25
% O	88.65	81.98	82.05	72.44
s/p/d	34.12/65.82/0.06	28.62/71.30/0.09	24.18/75.71/0.11	22.54/77.34/0.12
	5, $Fe(CO)_3(O_3)$	**6**, $Co(CO)_2(H)(O_3)$	**7**, $Ni(CO)_2(O_3)$	**8**, $Cu(CO)(H)(O_3)$
% M	32.23	42.26	24.97	99.60
s/p/d	16.38/0.08/83.54	0.02/0.15/99.82	18.29/2.03/79.68	0.01/0.21/99.78
% O	67.77	57.74	75.03	0.40
s/p/d	15.95/83.9/0.15	0.00/99.92/0.08	6.88/92.97/0.14	4.85/95.03/0.12

[a] Contribution of the atom to the bond orbital. [b] Hybridization percentages at atom center.

TABLE 8: Bond Dissociation Energies (D_e) of the M−O_3 Bond in $M(CO)_m(H)_n(O_3)$, Corrected for the Zero-Point Vibrational Energy (D_0) and the Basis Set Superposition Error (D_0^{BSSE})[a]

	1, $Ti(CO)_5(O_3)$	**2**, $V(CO)_4(H)(O_3)$	**3**, $Cr(CO)_4(O_3)$	**4**, $Mn(CO)_3(H)(O_3)$
D_e	86.7	88.3	67.1	74.3
D_0	85.8	85.7	65.5	72.3
D_0^{BSSE}	78.4	76.5	57.7	64.4
	5, $Fe(CO)_3(O_3)$	**6**, $Co(CO)_2(H)(O_3)$	**7**, $Ni(CO)_2(O_3)$	**8**, $Cu(CO)(H)(O_3)$
D_e	92.9	65.3	37.0	19.0
D_0	90.5	63.0	35.3	18.1
D_0^{BSSE}	82.1	55.4	27.5	12.1

[a] Energies in kcal/mol.

and the $V(CO)_4H$ unit can certainly be interpreted as "bonding" stabilizing interactions, but whether that is enough to constitute actual bonds may be debatable. From a chemical perspective, which is indeed one of the aims of NBO analysis, it becomes difficult to make sense of the results in the presence of such highly delocalizing contributions. Although it leads to a higher non-Lewis occupation, it was reasoned that to describe the bonding and learn something from the description, an explicit specification of a Lewis structure is needed and hence the resulting NBO partitioning was used in all of the remaining analyses.

Table 7 shows the results. Specifying the Lewis structure leads to Lewis orbital occupations between 91% and 96%. The metal−ozone bond orbital is largely polarized toward the ozone, as is expected from an interaction involving mainly ligand donation. An exception occurs in the Cu complex. Paradoxically, according to the NBO analysis, the antibonding orbital has a higher occupation than the bonding orbital! Therefore this orbital is listed in the table instead of its bonding counterpart. In all cases there is at least one antibonding M−O orbital of high occupation, but the Cu complex is the only one in which this orbital dominates the ligand to metal bonding.

As mentioned earlier, all complexes have significant 4s-orbital occupations, leading to ligand−metal bonds that have large sd^n-hybridization contributions on the metal. The first five complexes, **1**−**5**, show s-orbital mixing, consistent with the ozone ligand affecting charge transfer into the 4s-orbital of the metal that increases as the ligand environment of the metal becomes "more crowded" and d-orbital occupation increases, due to donation by non-ozone ligands. In the Co complex, **6**, only d-orbitals take part in the bonding, which is also the case in complex **8**. Both of these contain the H ligand used to satisfy the 18-electron rule, which interacts with the metal through an sd-hybrid, possibly causing little involvement of s-orbitals in the metal hybrid of the metal−ligand bond. Hybridization at the coordinating oxygen atoms contain largely sp-mixing, with the exception of complex **6**, which has solely p-orbital interaction.

Bond Dissociation Energies. Bond dissociation energies, corrected for the basis set superposition error (BSSE) by use of the counterpoise correction (CP),[34,35] and corrected for zero point vibrational energy (ZPVE) were also calculated. The fragments considered for the calculation of these properties were ground state free O_3 on the one hand, and $M(CO)_m(H)_n$ on the other. Both were taken in their neutral states, hence assuming that partial O_3 reduction and M oxidation take place upon complexation. This means that changes in energy values due to electron transfer are also intrinsically factored into the bond dissociation energies, increasing the values. The results are shown in Table 8. The BSSE corrections vary from 5.9 kcal/mol for Cu to 9.2 kcal/mol for V. The $Fe(CO)_3(O_3)$ complex has the highest D_0^{BSSE} value at 82.1 kcal/mol, followed by $Ti(CO)_5(O_3)$, 78.4 kcal/mol, and $V(CO)_4H(O_3)$, 76.5 kcal/mol. The $Cu(CO)H(O_3)$ complex has the lowest dissociation energy for the M−O_3 bond, 12.1 kcal/mol. The complete order of increasing bond dissociation energy is

Cu (**8**) < Ni (**7**) < Co (**6**) < Cr (**3**) < Mn (**4**) < V(**2**) < Ti (**1**) < Fe (**5**)

An important observation is that all complexes investigated have positive dissociation energies, indicating that ozone complexes with the first-row transition metals of the composition $M(CO)_m(H)_n(O_3)$ are viable and if synthesized should be stable.

Higher Valent Complexes. Finally, a few additional calculations were carried out to test the effect of the high reduction potential of ozone. Two representative complexes were thus calculated in higher oxidation states of +2 and +3, $[Cr(CO)_4(O_3)]^{2+/3+}$ and $[Fe(CO)_3(O_3)]^{2+/3+}$. Apart from the change in the M−O bond distances, a considerable decrease in the O−O bond length of the ozone ligands is observed with an increase in oxidation state. In $[Cr(CO)_4(O_3)]^{2+}$ the O−O bond length is 1.340 Å. The M−O bond distances are less sensitive and with the same complex show a smaller decrease of 0.05 Å. A stable structure for the $[Cr(CO)_4(O_3)]^{3+}$ complex could not be obtained. In $[Fe(CO)_3(O_3)]^{2+}$ the O−O separation is 1.286 Å, and in [Fe-

$(CO)_3(O_3)]^{3+}$ it is 1.278 Å. The M−O distance decreases in both these examples, by 0.136 and 0.190 Å, respectively (because an unsymmetrical structure is obtained for the +3 species, an average value is given for that complex). The higher oxidation state of the metal affects the ability of the ligand to be reduced upon complexation. This is reflected not only in the much shorter interatomic bond lengths of the ozone ligand but also in the sum of partial charges on the O_3 and metal centers, which remain positive.

IV. Conclusions

In this paper we have described the bonding and structures of complexes of first row transition metals with O_3, and supplemented with CO ligands. Bidentate complexes in which the terminal oxygens donate to the metal fragments are predicted for all examples, except Cu. The changes in structure of the O_3 fragment, partial atomic charges, as well as an investigation of the bond character with the CDA method, support a description of the metal fragments as being partially oxidized and the ligand reduced. In this description the ozone ligand forms a bond by donation to the d-orbitals of the metal, but back-donation by the metal fragment is then absent.

Unfortunately, the various criteria that were employed in this study as a measure of the strength of the interaction between the ozone ligand and the metal, i.e., bond length, electron density at critical points, amount of electron donation, and bond dissociation energies, do not give a consistent picture. The one exception is the Cu complex, which appears to be the least stable of all the complexes studied by any of the calculations. Cobalt and nickel, for example, have short metal−ozone bonds, relatively large electron density at the bond critical bonds, and a medium−high value for their electron donation parameters *d*. However, for both, the bond dissociation energy is among the lowest values calculated. By any of the criteria, V and Cr are always found somewhere in the middle of the trends observed. Bond dissociation energies indicate that the $Fe(CO)_3(O_3)$ complex is the most stable, and this complex also scores medium to high in the other tests. Ti has a high value for D_0 but is positioned low in the trend lines of other criteria. For the whole series investigated though, the bond dissociation energies indicate a considerable lowering in energy accompanying complexation and predict that transition metal complexes with ozone might soon be a reality. We are grateful to a referee for pointing out that another reason for the observed inconsistency might be the performance of the hybrid B3LYP functional as opposed to pure functionals, which often outperform a hybrid functional in transition metal species. However, given the lack of experimental results for verification of the computational values, there exists no a priori reason to mistrust the B3LYP findings.

Acknowledgment. This project was supported by the National Research Foundation of South Africa, grant number NRF2047216.

References and Notes

(1) Yamaguchi, Y.; Frisch, M. J.; Lee, T. J.; Schaefer, H. F., III; Binkley, J. S. *Theor. Chim. Acta* **1986**, *69*, 337.

(2) Xantheas, S. S.; Atchity, G. J.; Elbert, S. T.; Ruedenberg, K. *J. Chem. Phys.* **1991**, *94*, 8054.

(3) Wright, J. S. *Can. J. Chem.* **1973**, *51*, 139.

(4) Stanton, J. F.; Lipscomb, W. N.; Magers, D. H.; Bartlett, R. J. *J. Chem. Phys.* **1989**, *90*, 1077.

(5) Siebert, R.; Schinke, R.; Bitterová, M. *Phys. Chem. Chem. Phys.* **2001**, *3*, 1795.

(6) Scuseria, G. E.; Lee, T. J.; Scheiner, A. C.; Schaefer, H. F., III. *J. Chem. Phys.* **1989**, *90*, 5635.

(7) Murray, C. W.; Handy, N. C.; Amos, R. D. *J. Chem. Phys.* **1993**, *98*, 7145.

(8) Leininger, M. L.; Schaefer, H. F., III. *J. Chem. Phys.* **1997**, *107*, 9059.

(9) Lee, T. J. *J. Chem. Phys.* **1990**, *169*, 529.

(10) Lee, T. J.; Allen, W. D.; Schaefer, H. F., III. *J. Chem. Phys.* **1987**, *87*, 7062.

(11) Adler-Golden, S. M.; Langhoff, S. R.; Bauschlicher, C. W., Jr.; Carney, J. *J. Chem. Phys.* **1985**, *83*, 255.

(12) Cotton, F. A.; Wilkinson G. *Advanced Inorganic Chemistry*, 4th ed.; Wiley: New York, 1980.

(13) Flemmig, B.; Wolczanski, P. T.; Hoffmann, R. *J. Am. Chem. Soc.* **2005**, *127*, 1278.

(14) Sung, S.; Hoffmann, R. *J. Mol. Sci.* **1983**, *1*, 1.

(15) Frisch, M. J.; Trucks, G. W.; Schlegel, H. B.; Scuseria, G. E.; Robb, M. A.; Cheeseman, J. R.; Zakrzewski, V. G.; Montgomery, J. A., Jr.; Stratmann, R. E.; Burant, J. C.; Dapprich, S.; Millam, J. M.; Daniels, A. D.; Kudin, K. N.; Strain, M. C.; Farkas, O.; Tomasi, J.; Barone, V.; Cossi, M.; Cammi, R.; Menucci, B.; Pomelli, C.; Adamo, C.; Clifford, S.; Ochterski, J.; Petersson, G. A.; Ayala, P. Y.; Cui, Q.; Morokuma, K.; Malick, D. K.; Rabuck, A. D.; Raghavachari, K.; Foresman, J. B.; Cioslowski, J.; Ortiz, J. V.; Baboul, A. G.; Stefanov, B. B.; Liu, G.; Liashenko, A.; Piskorz, P.; Komaromi, I.; Gomperts, R.; Martin, R. L.; Fox, D. J.; Keith, T.; Al-Laham, M. A.; Peng, C. Y.; Nanayakkara, A.; Gonzalez, C.; Challocombe, M.; Gill, P. M. W.; Johnson, B.; Chen, W.; Wong, M. W.; Andres, J. L.; Head-Gordon, M.; Replogle, E. S.; Pople, J. A. *Gaussian 98*, revision A.7; Gaussian, Inc.: Pittsburgh, PA, 1998.

(16) Frisch, M. J.; Trucks, G. W.; Schlegel, H. B.; Scuseria, G. E.; Robb, M. A.; Cheeseman, J. R.; Montgomery, J. A., Jr.; Vreven, T.; Kudin, K. N.; Burant, J. C.; Millam, J. M.; Iyengar, S. S.; Tomasi, J.; Barone, V.; Menucci, B.; Cossi, M.; Scalmani, G.; Rega, N.; Petersson, G. A.; Nakatsuji, H.; Hada, M.; Ehara, M.; Toyota, K.; Fukuda, R.; Hasegawa, J.; Ishida, M.; Nakajima, T.; Hona, Y.; Kitao, O.; Nakai, H.; Klene, M.; Li, X.; Knox, J. E.; Hratchian, H. P.; Cross, J. B.; Adamo, C.; Jaramillo, J.; Gomperts, R.; Stratmann, R. E.; Yazyev, O.; Austin, A. J.; Cammi, R.; Pomelli, C.; Ochterski, J. W.; Ayala, P. Y.; Morokuma, K.; Voth, G. A.; Salvador, P.; Dannenberg, J. J.; Zakrzewski, V. G.; Dapprich, S.; Daniels, A. D.; Strain, M. C.; Farkas, O.; Malick, D. K.; Rabuck, A. D.; Raghavachari, K.; Foresman, J. B.; Ortiz, J. V.; Cui, Q.; Baboul, A. G.; Clifford, S.; Cioslowski, J.; Stefanov, B. B.; Liu, G.; Liashenko, A.; Piskorz, P.; Komaromi, I.; Martin, R. L.; Fox, D. J.; Keith, T.; Al-Laham, M. A.; Peng, C. Y.; Nanayakkara, A.; Challacombe, M.; Gill, P. M. W.; Johnson, B.; Chen, W.; Wong, M. W.; Gonzalez, A.; Pople, J. A. *Gaussian 03*, revision B.05; Gaussian, Inc.: Pittsburgh, PA, 2003.

(17) Becke, A. D. *J. Chem. Phys.* **1993**, *98*, 5648.

(18) Hay, P. J.; Wadt, W. R. *J. Chem. Phys.* **1985**, *82*, 299.

(19) Bauernschmitt, R.; Ahlrichs, R. *J. Chem. Phys.* **1996**, *104*, 9047.

(20) Seeger, R.; Pople, J. A. *J. Chem. Phys.* **1977**, *66*, 3045.

(21) Weinhold, F. In *Encyclopedia of Computational Chemistry*; v. R. Schleyer, P., Clark, T., Kollman, P. A., Schaefer, H. F., Scheiner, P. R., III, Eds.; Wiley-VCH: Chichester, U.K., 1998; Vol. 3, pp 1793.

(22) Reed, A. E.; Curtiss, L. A.; Weinhold, F. *Chem. Rev.* **1988**, *88*, 899.

(23) Bader, R. F. W. *Atoms in Molecules. A Quantum Theory*; Oxford University Press: Oxford, U.K., 1990.

(24) Biegler-König, F. W.; Bader, R. F. W. *J. Comput. Chem.* **1982**, *3*, 317.

(25) Chatt, J.; Duncanson, L. A. *J. Chem. Soc.* **1953**, 2939.

(26) Dewar, M. J. S. *Bull. Soc. Chim. Fe.* **1951**, *C71*, 18.

(27) Dapprich, S.; Frenking, G. CDA 2.1, Philipps-Universität Marburg, Marburg, Germany, http://www.chemie.uni-marburg.de/~frenking/cda/cda-.tar.gz.

(28) Dapprich, S.; Frenking, G. *J. Phys. Chem.* **1995**, *99*, 9352.

(29) Ehlers, A. W.; Dapprich, S.; Vyboishchikov, S. F.; Frenking, G. *Organometallics* **1996**, *15*, 105.

(30) (a) Wang, L. J.; Woo, S. B. *Phys. Rev. A* **1987**, *35*, 759. (b) Depannemaecker, J.-C.; Bellet, J. *J. Mol. Spectrosc.* **1977**, *66*, 106. (c) Colmont, J.-M.; Demaison, J.; Cosleou, J. *J. Mol. Spectrosc.* **1995**, *171*, 453−467. (d) Tyuterev, G., IV; Tashkun, S.; Jensen, P.; Barbe, A.; Cours, T. *J. Mol. Spectrosc.* **1999**, *198*, 57−76.

(31) Valentine, J. S. *Chem. Rev.* **1973**, *73*, 235.

(32) Frenking, G.; Frölich, N. *Chem. Rev.* **2000**, *100*, 717.

(33) Cremer, D.; Kraka, E. *Angew. Chem., Int. Ed.* **1984**, *23*, 627.

(34) Boys, S. F.; Bernardi, F. *Mol. Phys.* **1970**, *19*, 553.

(35) Van Duijneveldt, F. B.; Van Duijneveldt-van de Rijdt, J. G. C. M.; Van Lenthe, J. H. *Chem. Rev.* **1994**, *94*, 1873.